ELSEVIER

A mechanistic approach to tip-induced nano-lithography of polymer surfaces

J.A. Blach[a,b,]*, G.S. Watson[a], C.L. Brown[a,b], D.K. Pham[c], J. Wright[c], D.V. Nicolau[c], S. Myhra[a]

[a]*School of Science, Griffith University, Nathan, Queensland 4111, Australia*
[b]*CRC for MicroTechnology, Level 5, 60 William Street, Hawthorn, Victoria 3122, Australia*
[c]*Industrial Research Institute Swinburne, Swinburne University of Technology, P.O. Box 218, Hawthorn, Victoria 3122, Australia*

Abstract

Tip-induced lithography based on local probe methods is a contender for next-generation technologies that require spatially differentiated topographical and/or chemical manipulation of polymer surfaces on the nano-scale. The present project is based on force microscopy and has demonstrated topographical manipulation of P(tBuMA) at a line width of 20–30 nm. Lateral force analysis shows that the surface chemistry can also be manipulated with comparable spatial resolution. The present project has been concerned with establishing relationships between lithographic outcomes and tip shape, linear raster speed, out-of-plane normal force, and in-plane shear/friction force. Elements of 'ploughing', in combination with elastic recovery and chain scission appear to be necessary aspects of an explanatory model.
© 2003 Elsevier B.V. All rights reserved.

1. Introduction

The surface structure and chemistry of polymers affect their functionality for a range of applications in areas as diverse as biosensors, corrosion protection, semi-conductor processing, biofouling, tissue engineering and biomaterials technology. Some of those applications require purposeful tailoring of laterally differentiated regions (e.g. array structures for multi-channel/multi-analyte biosensors and patterning for promotion of selective adhesion of cells). While such tailoring is currently taking place on the micrometre-scale, it is likely in the future to progress into the nanometre-regime. Thus there is an evolving need for manipulation and characterisation of patterned surfaces, where AFM is a leading contender as a favoured processing tool. At present, the explanatory models for tip-induced manipulation of polymer surfaces is in an unsatisfactory state. Earlier studies have approached the problem from sev-

eral perspectives, generally based on insight gained from unrelated materials [1–6]. The principal objective of the present study is to explore the relative importance of the physico-chemical variables and parameters of the system, with a view to establishing mechanistic relationships.

Poly-*tert*-butylmethacrylate, P(tBuMA) has potential applications as a bio-active/selective polymer, and has been adopted as a topical system for investigation [7]. This study identifies conditions which result in the tip-induced structural and chemical alteration of the surface.

2. Experimental details

2.1. Materials preparation and processing and specimen configuration

A 5 wt.% solution of P(tBuMA) (Polysciences, Inc) in cyclohexane was spin-coated 3000 rev./min for 40 s onto a cover glass primed with hexamethyldisilazane (Sigma Aldrich Co.). The coated substrates were then soft baked at 90 °C for 30 min, and stored in a desiccator prior to use. The RMS surface roughness was deter-

*Corresponding author. Tel.: +61-7-3875-7531; fax: +61-7-3875-7656.
E-mail address: j.blach@griffith.edu.au (J.A. Blach).

mined by AFM; typical values were 4 and 2 nm for fields of view of 25×25 and 5×5 μm^2, respectively.

2.2. AFM instrumentation and probes

The work was carried out on a JEOL JSPM-4200 system with a 25 μm tube scanner, with a z-range of approximately 3 μm. The system is based on the detection of the tip-to-surface forces through monitoring deflection of a laser beam incident on a force-sensing/imposing lever. The analyses were carried out under air-ambient conditions (temperature of 23 °C and 65% relative humidity).

The probe consists of a lever and an integral tip. 'Diving-board' probes (NT-MDT Ultrasharp SC12C series) were used throughout the work. Typical parameters were: normal force constant, k_N, of 4.5 N/m; conical tip shape with cone angle $<20°$; radius of curvature of the tip <10 nm; and tip height of 10–15 μm. The actual normal force constant was determined from the resonance method [8], and the torsional force constant was calculated from the expression for a long and thin lever [9] [see Eq. (2) below].

2.3. Operational modes and image processing

The following subset of the capabilities of the AFM system was used during the present project.

Imaging: Topographical imaging was carried out at constant force in contact mode, with a lever-imposed normal force in the range 10–40 nN. The scanning rate in the fast-scan direction was approximately 3 Hz, and a typical image was composed of 500×500 pixels.

Lateral force analysis (*LFM*): 'Friction' loop analysis was carried out by monitoring the torsional deformation of the lever during forward and reverse line scans. The normal force and linear scan speed were then comparable to those for imaging.

Force vs. distance (*F-d*) *analysis*: The tip is held stationary at an $x-y$ (sample plane) location and is ramped along the z-axis, first in the direction of approach and contact with the surface, and then in the reverse direction.

Lithography: Lithographic patterning of the polymer was carried out by scanning the tip at a particular angle in relation to the fixed geometry of the lever. Specific parameters such as loading force, scan speed and tip shape are described below.

Topographical images were processed by subtraction of background and adjustment of brightness and contrast. Some images were enhanced through 3D-presentation and shading by a synthetic light source, while others are shown with grey-scale contrast. Other data reduction is described below.

3. Nano-mechanical considerations

Manipulation of soft surfaces such as polymers is likely to depend on both out-of-plane and in-plane forces acting at the point of contact between the tip and the polymer. Thus, quantification of the interactions will require a description of the deformational modes of the lever and tip, and their relationship to forces that are being 'sensed' and imposed by the probe. The expressions for force constants of deformation—arising from bending (k_N) and torsion (k_T)—are shown below [9]. The expressions assume that the deformation of the lever can be described by the lowest order modes of a long thin beam.

$$k_N = \frac{3EI}{L^3} \tag{1}$$

$$k_T = \frac{2EI}{(1+\mu)Lh^2} \tag{2}$$

where $E =$ Young's modulus, $\mu =$ Poisson's ratio, $I = wt^3/12$ is the reduced moment of inertia, $L =$ length of the lever, and $h =$ height of the tip. The k_T mode is stimulated by force components acting along the x-direction, referenced to a co-ordinate system anchored in the probe, with the y-axis aligned with the long axis of the lever.

4. Results and discussion

4.1. Polymer lithography—elastic recovery

Fig. 1 shows the results of carrying out single line scans, with the tip moving at a constant linear speed, but for different force loadings. Higher force loadings resulted in the formation of deeper troughs. At a loading of 60 nN the polymer undergoes plastic deformation with a line depth less than 1 nm and a line width of approximately 20 nm. The same tip was used to image the surface following the lithographic procedure. An *F–d* curve was obtained in order to determine the extent of quasi-static indentation as a function of force loading (Fig. 1g). The *F–d* data show that for a given normal force the static indentation is an order of magnitude greater than the depth of the trough arising from permanent deformation. For example, the *F–d* data show an indentation of 60–70 nm while the measured depth of the trough was approximately 6 nm (Fig. 1e). This observation suggests that the polymer will recover elastically up to 90% of the total dynamic deformation, while only some 10% of the original deformation will not recover.

4.2. Tip-induced alteration of surface chemistry

A rectangular pit of approximately 8 nm depth and 1×1 μm^2 area was excavated by a single raster. The

feature is shown in Fig. 2a. The lever was aligned with the *x*-axis while the fast-scan direction was along the *y*-axis. The image shows that the excavated material was preferentially deposited at the edges perpendicular to the fast scan direction (i.e. when the tip was stationary). Lateral force analysis revealed that the 'friction' inside the pit was lower than on the original surface, Fig. 2b. A friction contrast represents laterally differentiated surface chemistry. Thus the effect of tip-induced surface manipulation is to alter the surface chemistry, presumably due to chain scission.

4.3. Shear forces and ploughing

The line profiles in Fig. 1 show that the excavated material is deposited along the length of a trench, while the image in Fig. 2 shows that the material can be deposited at the end of a trace where the tip reverses direction and is momentarily stationary. Those observations are consistent with there being a contribution from a ploughing mechanism. The lever is generally tilted with respect to the horizontal, by 10° in the present case, in order to meet the requirements for optimal performance of the optical detection system. In the case when the opening half-angle of the cone is 10°, the forward and reverse angles of attack, (referenced to the normal to the surface), of the tip will then be 0 and 20°, respectively. The angle is 10° when the scan direction is perpendicular. The results obtained from inscribing linear trenches revealed that the lateral force increased with decreasing angle of attack, but that the lithographic efficiency decreased (less material excavated). Fig. 3 shows the dependence of the lithographic
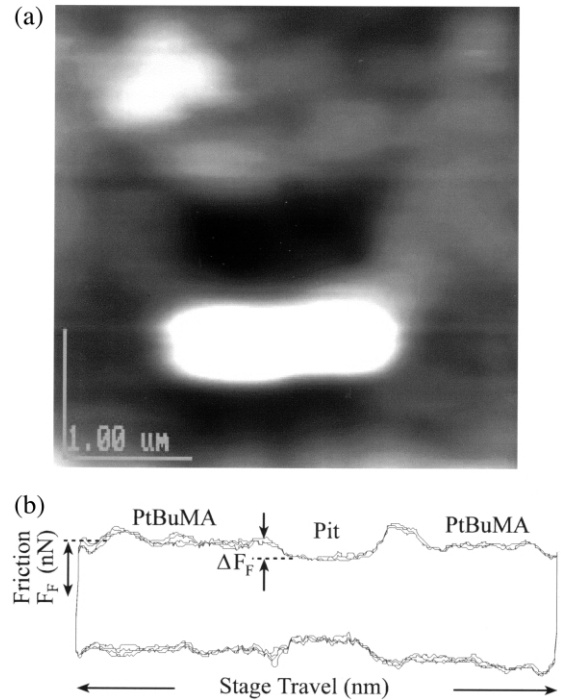

Fig. 2. (a) Topographic image of pit arising from rastering at a normal force of 1 μN. (b) The trace represents four repeat line scans across the field of view in (a) along the *y*-axis. A lower lateral force was observed when the tip traversed the region of the pit.

efficiency, in terms of the cross-section of the trench, vs. the angle of attack, and the ratio of shear force to loading force.

The relationships between extent of removal of material, lateral force and normal force are shown in Fig. 4.
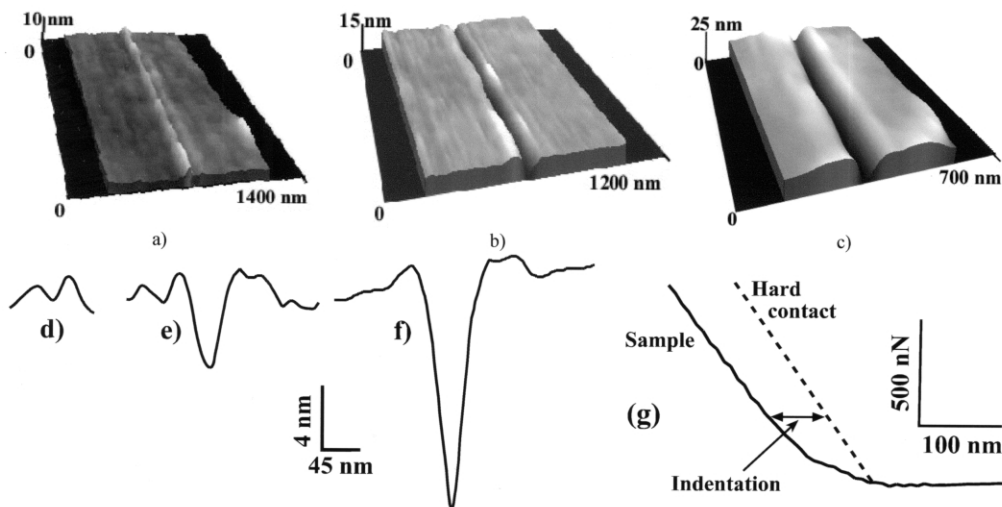

Fig. 1. (a–c) Topographic images of P(tBuMA) surfaces after single line scans (with the long axis of the lever aligned with the scan direction). (d–f) Corresponding line profiles for lever-induced normal force loadings of 60, 260 and 450 nN. The linear scan speed was held constant at 100 μm/s. (g) The *F–d* curve shows extent of quasi-static tip indentation as a function of force loading (the 'hard' contact calibration curve was obtained from the glass substrate).
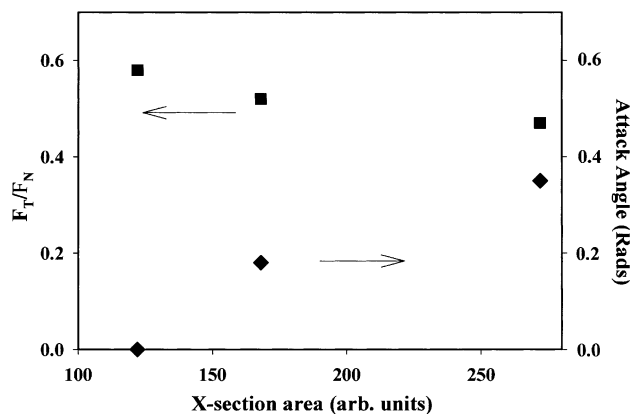
Fig. 3. The relationships between the cross-sectional area of the trench, the angle of attack (diamond symbols) (in radians), and the ratio of shear force to normal force (square symbols) (F_T/F_N). The normal force and scan speed were maintained constant at 850 nN and 10 μm/s, respectively.

Fig. 4. The relationships between material removed, along horizontal axis, and normal force (filled symbols) and lateral force (open symbols) acting on the lever. The measure of removed material is essentially the cross-sectional area of a trench (depth×width in nm²). The linear tip speed was 10 μm/s and the lever was characterised by $k_N = 4.6$ N/m. The length of each trench was 3–5 μm.

The dependence is non-linear and suggests that a minimum force is required in order to initiate removal of material. However, within the experimental accuracy there was a linear relationship between normal and lateral force components.

4.4. Nano-machining of P(tBuMA)

An example of tip-induced nano-machining is shown in Fig. 5. The material that was initially excavated from the wells was deposited along the edges. However, subsequent scanning over a larger field of view at lower force loading removed the material from the edges indicating that it is was loosely bound to the surface.

The structure shown in Fig. 5 was re-imaged after 100 h; there was no apparent change in height or size of the structure. Accordingly, any long-term elastic recovery was below the level of detectability.

5. Conclusions

It has been shown that AFM modification of a bioactive polymer (P(tBuMA)) can produce 3-dimensional structures at a spatial resolution corresponding to line width and depth less than 20 nm and 1 nm, respectively. The process is a reliable means of producing surface features on the nano-scale. The use of AFM
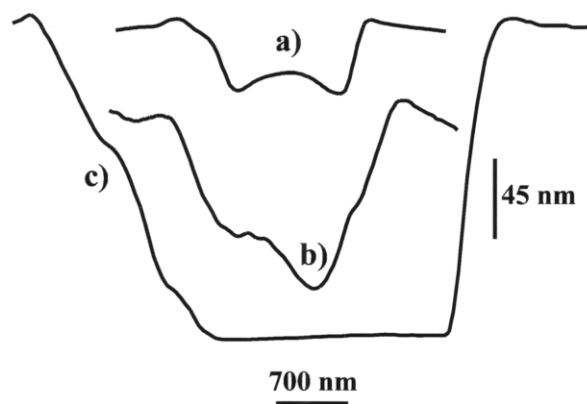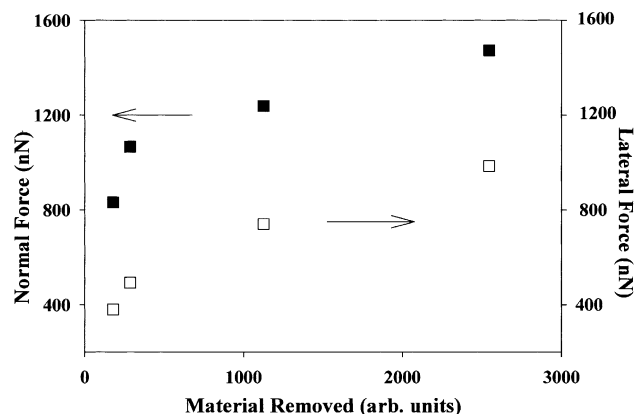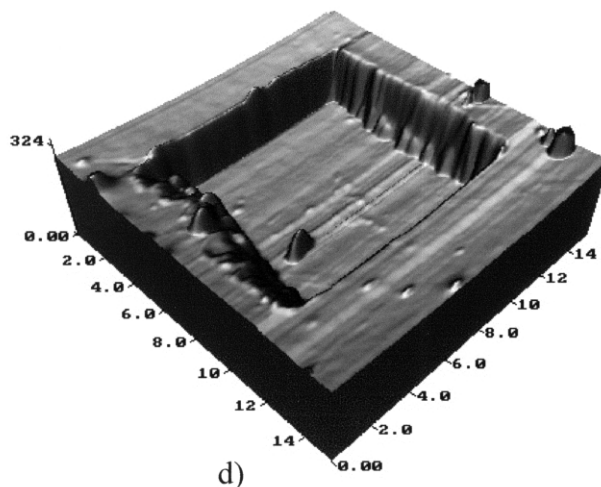

Fig. 5. The line profiles (a–c) show the outcomes of manipulating the polymer surface by a series of raster scans: (a) 680 nN and two rasters, (b) 870 nN and three rasters, and (c) 680 nN and seven rasters. The linear scan speed was 350 μm/s. (d) A topographic image in 3D representation of the final feature.

in comparison with other lithographic techniques such as electron-beam or UV treatment provides greater spatial resolution and eliminates proximity effects. As well, the process avoids the effects of the deposition of direct ionising and thermal radiation. The results show that an explanatory model will require elements from several mechanisms—including elastic recovery, chain scission and ploughing.

Acknowledgments

References

[1] L.G. Hector, S.R. Schmid, Wear 215 (1998) 247.
[2] S.R. Schmid, L.G. Hector, Wear 215 (1998) 257.
[3] T-H. Fang, C-I. Weng, J-G. Chang, Nanotechnology 11 (2000) 181.
[4] B. Bhushan, Wear 251 (2001) 1105.
[5] J.P. Pickering, G.J. Vancso, Appl. Surf. Sci. 148 (1999) 147.
[6] B. Cappella, H. Sturm, S.M. Weidner, Polymer 43 (2002) 4461.
[7] G.S. Watson, J.A. Blach, D.V. Nicolau, D.K. Pham, J. Wright, S. Myhra, Polym. Int. (2003) in press.
[8] J.P. Cleveland, S. Manne, D. Bocek, P.K. Hansma, Rev. Sci. Instrum. 64 (1993) 403.
[9] C.T. Gibson, G.S. Watson, S. Myhra, Scanning 19 (1997) 564.